

This is the accepted manuscript made available via CHORUS. The article has been published as:

Measurement of the forward-backward asymmetry of Λ and $\Lambda[\text{over } \bar{}]$ production in $pp[\text{over } \bar{}]$ collisions

V. M. Abazov *et al.* (D0 Collaboration)

Phys. Rev. D **93**, 032002 — Published 9 February 2016

DOI: [10.1103/PhysRevD.93.032002](https://doi.org/10.1103/PhysRevD.93.032002)

Measurement of the forward-backward asymmetry of Λ and $\bar{\Lambda}$ production in $p\bar{p}$ collisions

V.M. Abazov,³¹ B. Abbott,⁶⁷ B.S. Acharya,²⁵ M. Adams,⁴⁶ T. Adams,⁴⁴ J.P. Agnew,⁴¹ G.D. Alexeev,³¹ G. Alkhazov,³⁵ A. Alton^{a, 56} A. Askew,⁴⁴ S. Atkins,⁵⁴ K. Augsten,⁷ C. Avila,⁵ F. Badaud,¹⁰ L. Bagby,⁴⁵ B. Baldin,⁴⁵ D.V. Bandurin,⁷⁴ S. Banerjee,²⁵ E. Barberis,⁵⁵ P. Baringer,⁵³ J.F. Bartlett,⁴⁵ U. Bassler,¹⁵ V. Bazterra,⁴⁶ A. Bean,⁵³ M. Begalli,² L. Bellantoni,⁴⁵ S.B. Beri,²³ G. Bernardi,¹⁴ R. Bernhard,¹⁹ I. Bertram,³⁹ M. Besançon,¹⁵ R. Beuselinck,⁴⁰ P.C. Bhat,⁴⁵ S. Bhatia,⁵⁸ V. Bhatnagar,²³ G. Blazey,⁴⁷ S. Blessing,⁴⁴ K. Bloom,⁵⁹ A. Boehnlein,⁴⁵ D. Boline,⁶⁴ E.E. Boos,³³ G. Borissov,³⁹ M. Borysova^{l, 38} A. Brandt,⁷¹ O. Brandt,²⁰ R. Brock,⁵⁷ A. Bross,⁴⁵ D. Brown,¹⁴ X.B. Bu,⁴⁵ M. Buehler,⁴⁵ V. Buescher,²¹ V. Bunichev,³³ S. Burdin^{b, 39} C.P. Buszello,³⁷ E. Camacho-Pérez,²⁸ B.C.K. Casey,⁴⁵ H. Castilla-Valdez,²⁸ S. Caughron,⁵⁷ S. Chakrabarti,⁶⁴ K.M. Chan,⁵¹ A. Chandra,⁷³ E. Chapon,¹⁵ G. Chen,⁵³ S.W. Cho,²⁷ S. Choi,²⁷ B. Choudhary,²⁴ S. Cihangir,⁴⁵ D. Claes,⁵⁹ J. Clutter,⁵³ M. Cooke^{k, 45} W.E. Cooper,⁴⁵ M. Corcoran,⁷³ F. Couderc,¹⁵ M.-C. Cousinou,¹² J. Cuth,²¹ D. Cutts,⁷⁰ A. Das,⁷² G. Davies,⁴⁰ S.J. de Jong,^{29, 30} E. De La Cruz-Burelo,²⁸ F. Déliot,¹⁵ R. Demina,⁶³ D. Denisov,⁴⁵ S.P. Denisov,³⁴ S. Desai,⁴⁵ C. Deterre^{c, 41} K. DeVaughan,⁵⁹ H.T. Diehl,⁴⁵ M. Diesburg,⁴⁵ P.F. Ding,⁴¹ A. Dominguez,⁵⁹ A. Dubey,²⁴ L.V. Dudko,³³ A. Duperrin,¹² S. Dutt,²³ M. Eads,⁴⁷ D. Edmunds,⁵⁷ J. Ellison,⁴³ V.D. Elvira,⁴⁵ Y. Enari,¹⁴ H. Evans,⁴⁹ A. Evdokimov,⁴⁶ V.N. Evdokimov,³⁴ A. Fauré,¹⁵ L. Feng,⁴⁷ T. Ferbel,⁶³ F. Fiedler,²¹ F. Filthaut,^{29, 30} W. Fisher,⁵⁷ H.E. Fisk,⁴⁵ M. Fortner,⁴⁷ H. Fox,³⁹ J. Franc,⁷ S. Fuess,⁴⁵ P.H. Garbincius,⁴⁵ A. Garcia-Bellido,⁶³ J.A. García-González,²⁸ V. Gavrilov,³² W. Geng,^{12, 57} C.E. Gerber,⁴⁶ Y. Gershtein,⁶⁰ G. Ginther,⁴⁵ O. Gogota,³⁸ G. Golovanov,³¹ P.D. Grannis,⁶⁴ S. Greder,¹⁶ H. Greenlee,⁴⁵ G. Grenier,¹⁷ Ph. Gris,¹⁰ J.-F. Grivaz,¹³ A. Grohsjean^{c, 15} S. Grünendahl,⁴⁵ M.W. Grünewald,²⁶ T. Guillemain,¹³ G. Gutierrez,⁴⁵ P. Gutierrez,⁶⁷ J. Haley,⁶⁸ L. Han,⁴ K. Harder,⁴¹ A. Harel,⁶³ J.M. Hauptman,⁵² J. Hays,⁴⁰ T. Head,⁴¹ T. Hebbeker,¹⁸ D. Hedin,⁴⁷ H. Hegab,⁶⁸ A.P. Heinson,⁴³ U. Heintz,⁷⁰ C. Hensel,¹ I. Heredia-De La Cruz^{d, 28} K. Herner,⁴⁵ G. Hesketh^{f, 41} M.D. Hildreth,⁵¹ R. Hirosky,⁷⁴ T. Hoang,⁴⁴ J.D. Hobbs,⁶⁴ B. Hoeneisen,⁹ J. Hogan,⁷³ M. Hohlfeld,²¹ J.L. Holzbauer,⁵⁸ I. Howley,⁷¹ Z. Hubacek,^{7, 15} V. Hynek,⁷ I. Iashvili,⁶² Y. Ilchenko,⁷² R. Illingworth,⁴⁵ A.S. Ito,⁴⁵ S. Jabeen^{m, 45} M. Jaffré,¹³ A. Jayasinghe,⁶⁷ M.S. Jeong,²⁷ R. Jesik,⁴⁰ P. Jiang,⁴ K. Johns,⁴² E. Johnson,⁵⁷ M. Johnson,⁴⁵ A. Jonckheere,⁴⁵ P. Jonsson,⁴⁰ J. Joshi,⁴³ A.W. Jung^{o, 45} A. Juste,³⁶ E. Kajfasz,¹² D. Karmanov,³³ I. Katsanos,⁵⁹ M. Kaur,²³ R. Kehoe,⁷² S. Kermiche,¹² N. Khalatyan,⁴⁵ A. Khanov,⁶⁸ A. Kharchilava,⁶² Y.N. Kharzheev,³¹ I. Kiselevich,³² J.M. Kohli,²³ A.V. Kozelov,³⁴ J. Kraus,⁵⁸ A. Kumar,⁶² A. Kupco,⁸ T. Kurča,¹⁷ V.A. Kuzmin,³³ S. Lammers,⁴⁹ P. Lebrun,¹⁷ H.S. Lee,²⁷ S.W. Lee,⁵² W.M. Lee,⁴⁵ X. Lei,⁴² J. Lellouch,¹⁴ D. Li,¹⁴ H. Li,⁷⁴ L. Li,⁴³ Q.Z. Li,⁴⁵ J.K. Lim,²⁷ D. Lincoln,⁴⁵ J. Linnemann,⁵⁷ V.V. Lipaev,³⁴ R. Lipton,⁴⁵ H. Liu,⁷² Y. Liu,⁴ A. Lobodenko,³⁵ M. Lokajicek,⁸ R. Lopes de Sa,⁴⁵ R. Luna-Garcia^{g, 28} A.L. Lyon,⁴⁵ A.K.A. Maciel,¹ R. Madar,¹⁹ R. Magaña-Villalba,²⁸ S. Malik,⁵⁹ V.L. Malyshev,³¹ J. Mansour,²⁰ J. Martínez-Ortega,²⁸ R. McCarthy,⁶⁴ C.L. McGivern,⁴¹ M.M. Meijer,^{29, 30} A. Melnitchouk,⁴⁵ D. Menezes,⁴⁷ P.G. Mercadante,³ M. Merkin,³³ A. Meyer,¹⁸ J. Meyer^{i, 20} F. Miconi,¹⁶ N.K. Mondal,²⁵ M. Mulhearn,⁷⁴ E. Nagy,¹² M. Narain,⁷⁰ R. Nayyar,⁴² H.A. Neal,⁵⁶ J.P. Negret,⁵ P. Neustroev,³⁵ H.T. Nguyen,⁷⁴ T. Nunnemann,²² J. Orduna,⁷³ N. Osman,¹² J. Osta,⁵¹ A. Pal,⁷¹ N. Parashar,⁵⁰ V. Parihar,⁷⁰ S.K. Park,²⁷ R. Partridge^{e, 70} N. Parua,⁴⁹ A. Patwa^{j, 65} B. Penning,⁴⁰ M. Perfilov,³³ Y. Peters,⁴¹ K. Petridis,⁴¹ G. Petrillo,⁶³ P. Pétroff,¹³ M.-A. Pleier,⁶⁵ V.M. Podstavkov,⁴⁵ A.V. Popov,³⁴ M. Prewitt,⁷³ D. Price,⁴¹ N. Prokopenko,³⁴ J. Qian,⁵⁶ A. Quadt,²⁰ B. Quinn,⁵⁸ P.N. Ratoff,³⁹ I. Razumov,³⁴ I. Ripp-Baudot,¹⁶ F. Rizatdinova,⁶⁸ M. Rominsky,⁴⁵ A. Ross,³⁹ C. Royon,⁸ P. Rubinov,⁴⁵ R. Ruchti,⁵¹ G. Sajot,¹¹ A. Sánchez-Hernández,²⁸ M.P. Sanders,²² A.S. Santos^{h, 1} G. Savage,⁴⁵ M. Savitskiy,³⁸ L. Sawyer,⁵⁴ T. Scanlon,⁴⁰ R.D. Schamberger,⁶⁴ Y. Scheglov,³⁵ H. Schellman,^{69, 48} M. Schott,²¹ C. Schwanenberger,⁴¹ R. Schwienhorst,⁵⁷ J. Sekaric,⁵³ H. Severini,⁶⁷ E. Shabalina,²⁰ V. Shary,¹⁵ S. Shaw,⁴¹ A.A. Shchukin,³⁴ V. Simak,⁷ P. Skubic,⁶⁷ P. Slattery,⁶³ D. Smirnov,⁵¹ G.R. Snow,⁵⁹ J. Snow,⁶⁶ S. Snyder,⁶⁵ S. Söldner-Rembold,⁴¹ L. Sonnenschein,¹⁸ K. Soustruznik,⁶ J. Stark,¹¹ D.A. Stoyanova,³⁴ M. Strauss,⁶⁷ L. Suter,⁴¹ P. Svoisky,⁶⁷ M. Titov,¹⁵ V.V. Tokmenin,³¹ Y.-T. Tsai,⁶³ D. Tsybychev,⁶⁴ B. Tuchming,¹⁵ C. Tully,⁶¹ L. Uvarov,³⁵ S. Uvarov,³⁵ S. Uzunyan,⁴⁷ R. Van Kooten,⁴⁹ W.M. van Leeuwen,²⁹ N. Varelas,⁴⁶ E.W. Varnes,⁴² I.A. Vasilyev,³⁴ A.Y. Verkheev,³¹ L.S. Vertogradov,³¹ M. Verzocchi,⁴⁵ M. Vesterinen,⁴¹ D. Vilanova,¹⁵ P. Vokac,⁷ H.D. Wahl,⁴⁴ M.H.L.S. Wang,⁴⁵ J. Warchol,⁵¹ G. Watts,⁷⁵ M. Wayne,⁵¹ J. Weichert,²¹ L. Welty-Rieger,⁴⁸ M.R.J. Williams^{n, 49} G.W. Wilson,⁵³ M. Wobisch,⁵⁴ D.R. Wood,⁵⁵ T.R. Wyatt,⁴¹ Y. Xie,⁴⁵ R. Yamada,⁴⁵ S. Yang,⁴ T. Yasuda,⁴⁵ Y.A. Yatsunenko,³¹ W. Ye,⁶⁴ Z. Ye,⁴⁵ H. Yin,⁴⁵ K. Yip,⁶⁵ S.W. Youn,⁴⁵

J.M. Yu,⁵⁶ J. Zennaro,⁶² T.G. Zhao,⁴¹ B. Zhou,⁵⁶ J. Zhu,⁵⁶ M. Zielinski,⁶³ D. Zieminska,⁴⁹ and L. Zivkovic¹⁴

(The D0 Collaboration*)

¹LAFEX, Centro Brasileiro de Pesquisas Físicas, Rio de Janeiro, Brazil

²Universidade do Estado do Rio de Janeiro, Rio de Janeiro, Brazil

³Universidade Federal do ABC, Santo André, Brazil

⁴University of Science and Technology of China, Hefei, People's Republic of China

⁵Universidad de los Andes, Bogotá, Colombia

⁶Charles University, Faculty of Mathematics and Physics,

Center for Particle Physics, Prague, Czech Republic

⁷Czech Technical University in Prague, Prague, Czech Republic

⁸Institute of Physics, Academy of Sciences of the Czech Republic, Prague, Czech Republic

⁹Universidad San Francisco de Quito, Quito, Ecuador

¹⁰LPC, Université Blaise Pascal, CNRS/IN2P3, Clermont, France

¹¹LPSC, Université Joseph Fourier Grenoble 1, CNRS/IN2P3,

Institut National Polytechnique de Grenoble, Grenoble, France

¹²CPPM, Aix-Marseille Université, CNRS/IN2P3, Marseille, France

¹³LAL, Université Paris-Sud, CNRS/IN2P3, Orsay, France

¹⁴LPNHE, Universités Paris VI and VII, CNRS/IN2P3, Paris, France

¹⁵CEA, Irfu, SPP, Saclay, France

¹⁶IPHC, Université de Strasbourg, CNRS/IN2P3, Strasbourg, France

¹⁷IPNL, Université Lyon 1, CNRS/IN2P3, Villeurbanne, France and Université de Lyon, Lyon, France

¹⁸III. Physikalisches Institut A, RWTH Aachen University, Aachen, Germany

¹⁹Physikalisches Institut, Universität Freiburg, Freiburg, Germany

²⁰II. Physikalisches Institut, Georg-August-Universität Göttingen, Göttingen, Germany

²¹Institut für Physik, Universität Mainz, Mainz, Germany

²²Ludwig-Maximilians-Universität München, München, Germany

²³Punjab University, Chandigarh, India

²⁴Delhi University, Delhi, India

²⁵Tata Institute of Fundamental Research, Mumbai, India

²⁶University College Dublin, Dublin, Ireland

²⁷Korea Detector Laboratory, Korea University, Seoul, Korea

²⁸CINVESTAV, Mexico City, Mexico

²⁹Nikhef, Science Park, Amsterdam, the Netherlands

³⁰Radboud University Nijmegen, Nijmegen, the Netherlands

³¹Joint Institute for Nuclear Research, Dubna, Russia

³²Institute for Theoretical and Experimental Physics, Moscow, Russia

³³Moscow State University, Moscow, Russia

³⁴Institute for High Energy Physics, Protvino, Russia

³⁵Petersburg Nuclear Physics Institute, St. Petersburg, Russia

³⁶Institució Catalana de Recerca i Estudis Avançats (ICREA) and Institut de Física d'Altes Energies (IFAE), Barcelona, Spain

³⁷Uppsala University, Uppsala, Sweden

³⁸Taras Shevchenko National University of Kyiv, Kiev, Ukraine

³⁹Lancaster University, Lancaster LA1 4YB, United Kingdom

⁴⁰Imperial College London, London SW7 2AZ, United Kingdom

⁴¹The University of Manchester, Manchester M13 9PL, United Kingdom

⁴²University of Arizona, Tucson, Arizona 85721, USA

⁴³University of California Riverside, Riverside, California 92521, USA

⁴⁴Florida State University, Tallahassee, Florida 32306, USA

⁴⁵Fermi National Accelerator Laboratory, Batavia, Illinois 60510, USA

⁴⁶University of Illinois at Chicago, Chicago, Illinois 60607, USA

⁴⁷Northern Illinois University, DeKalb, Illinois 60115, USA

⁴⁸Northwestern University, Evanston, Illinois 60208, USA

⁴⁹Indiana University, Bloomington, Indiana 47405, USA

⁵⁰Purdue University Calumet, Hammond, Indiana 46323, USA

⁵¹University of Notre Dame, Notre Dame, Indiana 46556, USA

⁵²Iowa State University, Ames, Iowa 50011, USA

⁵³University of Kansas, Lawrence, Kansas 66045, USA

⁵⁴Louisiana Tech University, Ruston, Louisiana 71272, USA

⁵⁵Northeastern University, Boston, Massachusetts 02115, USA

⁵⁶University of Michigan, Ann Arbor, Michigan 48109, USA

⁵⁷Michigan State University, East Lansing, Michigan 48824, USA

⁵⁸University of Mississippi, University, Mississippi 38677, USA

⁵⁹University of Nebraska, Lincoln, Nebraska 68588, USA

- ⁶⁰Rutgers University, Piscataway, New Jersey 08855, USA
⁶¹Princeton University, Princeton, New Jersey 08544, USA
⁶²State University of New York, Buffalo, New York 14260, USA
⁶³University of Rochester, Rochester, New York 14627, USA
⁶⁴State University of New York, Stony Brook, New York 11794, USA
⁶⁵Brookhaven National Laboratory, Upton, New York 11973, USA
⁶⁶Langston University, Langston, Oklahoma 73050, USA
⁶⁷University of Oklahoma, Norman, Oklahoma 73019, USA
⁶⁸Oklahoma State University, Stillwater, Oklahoma 74078, USA
⁶⁹Oregon State University, Corvallis, Oregon 97331, USA
⁷⁰Brown University, Providence, Rhode Island 02912, USA
⁷¹University of Texas, Arlington, Texas 76019, USA
⁷²Southern Methodist University, Dallas, Texas 75275, USA
⁷³Rice University, Houston, Texas 77005, USA
⁷⁴University of Virginia, Charlottesville, Virginia 22904, USA
⁷⁵University of Washington, Seattle, Washington 98195, USA

We study Λ and $\bar{\Lambda}$ production asymmetries in $p\bar{p} \rightarrow \Lambda(\bar{\Lambda})X$, $p\bar{p} \rightarrow J/\psi\Lambda(\bar{\Lambda})X$, and $p\bar{p} \rightarrow \mu^\pm\Lambda(\bar{\Lambda})X$ events recorded by the D0 detector at the Fermilab Tevatron collider at $\sqrt{s} = 1.96$ TeV. We find an excess of Λ 's ($\bar{\Lambda}$'s) produced in the proton (antiproton) direction. This forward-backward asymmetry is measured as a function of rapidity. We confirm that the $\bar{\Lambda}/\Lambda$ production ratio, measured by several experiments with various targets and a wide range of energies, is a universal function of “rapidity loss”, i.e., the rapidity difference of the beam proton and the lambda.

PACS numbers: 13.85.Ni, 13.60.Rj

I. INTRODUCTION

We study $p\bar{p}$ collisions at a total center-of-mass energy $\sqrt{s} = 1.96$ TeV. Among the particles produced in these collisions are Λ 's and $\bar{\Lambda}$'s. In this paper we examine the question of whether the Λ and $\bar{\Lambda}$ retain some memory of the proton and antiproton beam directions. We consider the picture in which a strange quark produced directly in the hard scattering of point-like partons, or indirectly in the subsequent showering, can coalesce with a diquark remnant of the beam to produce a lambda particle, with the probability increasing with decreasing rapidity difference between the proton and the lambda [1–4].

The data were recorded in the D0 detector [5–9] at the Fermilab Tevatron collider. The full data set of 10.4 fb^{-1} , collected from 2002 to 2011, is analyzed. We choose a coordinate system in which the z axis is aligned with the proton beam direction and define the rapidity

TABLE I: Number of reconstructed Λ plus $\bar{\Lambda}$ or K_S with $p_T > 2.0$ GeV in each data set.

Data set	Number of events
(i) $p\bar{p} \rightarrow \Lambda(\bar{\Lambda})X$	5.85×10^5
(ii) $p\bar{p} \rightarrow J/\psi\Lambda(\bar{\Lambda})X$	2.50×10^5
(iii) $p\bar{p} \rightarrow \mu^\pm\Lambda(\bar{\Lambda})X$	1.15×10^7
(i) $p\bar{p} \rightarrow K_S X$	2.33×10^6
(ii) $p\bar{p} \rightarrow J/\psi K_S X$	6.55×10^5
(iii) $p\bar{p} \rightarrow \mu^\pm K_S X$	5.34×10^7

$y \equiv \frac{1}{2} \ln [(E + p_z)/(E - p_z)]$, where p_z is the outgoing particle momentum component in the z direction, and E is its energy, both in the $p\bar{p}$ center-of-mass frame. We measure the “forward-backward asymmetry” A_{FB} , i.e. the relative excess of Λ 's ($\bar{\Lambda}$'s) with longitudinal momentum in the p (\bar{p}) direction, as a function of $|y|$. The measurements include Λ 's and $\bar{\Lambda}$'s from all sources either directly produced or decay products of heavier hadrons.

The Λ 's ($\bar{\Lambda}$'s) are defined as “forward” if their longitudinal momentum is in the p (\bar{p}) direction. The asymmetry A_{FB} is defined as

$$A_{FB} \equiv \frac{\sigma_F(\Lambda) - \sigma_B(\Lambda) + \sigma_F(\bar{\Lambda}) - \sigma_B(\bar{\Lambda})}{\sigma_F(\Lambda) + \sigma_B(\Lambda) + \sigma_F(\bar{\Lambda}) + \sigma_B(\bar{\Lambda})}, \quad (1)$$

where $\sigma_F(\Lambda)$ and $\sigma_B(\Lambda)$ [$\sigma_F(\bar{\Lambda})$ and $\sigma_B(\bar{\Lambda})$] are the forward and backward cross sections of Λ [$\bar{\Lambda}$] production.

II. DETECTOR AND DATA

The D0 detector is described in Refs. [5–9]. The collision region is surrounded by a central tracking system

*with visitors from ^aAugustana College, Sioux Falls, SD, USA, ^bThe University of Liverpool, Liverpool, UK, ^cDESY, Hamburg, Germany, ^dCONACyT, Mexico City, Mexico, ^eSLAC, Menlo Park, CA, USA, ^fUniversity College London, London, UK, ^gCentro de Investigacion en Computacion - IPN, Mexico City, Mexico, ^hUniversidade Estadual Paulista, São Paulo, Brazil, ⁱKarlsruher Institut für Technologie (KIT) - Steinbuch Centre for Computing (SCC), D-76128 Karlsruhe, Germany, ^jOffice of Science, U.S. Department of Energy, Washington, D.C. 20585, USA, ^kAmerican Association for the Advancement of Science, Washington, D.C. 20005, USA, ^lKiev Institute for Nuclear Research, Kiev, Ukraine, ^mUniversity of Maryland, College Park, MD 20742, USA, ⁿEuropean Organization for Nuclear Research (CERN), Geneva, Switzerland and ^oPurdue University, West Lafayette, IN 47907, USA.

that comprises a silicon micro-strip vertex detector and a central fiber tracker, both located within a 1.9 T superconducting solenoidal magnet [5], surrounded successively by the liquid argon-uranium calorimeters, layer A of the muon system [6] (with drift chambers and scintillation trigger counters), the 1.8 T magnetized iron toroids, and two similar muon detector layers B and C after the toroids. The designs are optimized for vertex finding, tracking, and muon triggering and identification at pseudorapidities $|\eta|$ less than 2.5, 3.0, and 2.0 respectively. Pseudorapidity is defined as $\eta = -\ln \tan(\theta/2)$, where θ is the polar angle with respect to the proton beam direction.

We study three data sets: (i) $p\bar{p} \rightarrow \Lambda(\bar{\Lambda})X$, (ii) $p\bar{p} \rightarrow J/\psi\Lambda(\bar{\Lambda})X$, and (iii) $p\bar{p} \rightarrow \mu^\pm\Lambda(\bar{\Lambda})X$, and corresponding control samples with K_S instead of Λ or $\bar{\Lambda}$. Data set (i) is collected with a prescaled trigger on beam crossing (“zero bias events”) or with a prescaled trigger on energy deposited in forward luminosity counters (“minimum bias events”). Data set (ii) is selected with a suite of single muon, dimuon, and dedicated J/ψ triggers, from which $J/\psi \rightarrow \mu^+\mu^-$ candidates in association with a Λ or $\bar{\Lambda}$ are reconstructed. Data set (iii) is selected with a suite of single muon triggers, and a μ and a Λ are fully reconstructed offline. Data set (i) is unbiased, while most events in data sets (ii) and (iii) contain heavy quarks b or c [10, 11]. Data set (iii) has the same muon triggers and muon selections as in Refs. [10, 11]. In particular, the muons are required to have a momentum transverse to the beams $p_T > 4.2$ GeV or $p_z > 5.4$ GeV in order to traverse the central or forward iron toroid magnets. The number of reconstructed Λ plus $\bar{\Lambda}$ or K_S in each data sample is summarized in Table I. There is no strong physics reason to require a J/ψ or μ in an event: data sets (ii) and (iii) are analyzed because they are collected with muon or J/ψ triggers, and therefore are available and well understood, and data set (iii) is very large. The overlaps of the three data sets are negligible.

The Λ ’s, $\bar{\Lambda}$ ’s, and K_S ’s are reconstructed from pairs of oppositely charged tracks with a common vertex (V^0). Each track is required to have a non-zero impact parameter in the transverse plane (IP) with respect to the primary $p\bar{p}$ vertex with a significance of at least two standard deviations, and the V^0 projected to its point of closest approach is required to have an IP significance less than three standard deviations. The distance in the transverse plane from the primary $p\bar{p}$ vertex to the V^0 vertex is required to be greater than 4 mm. The V^0 is required to have $2.0 < p_T < 25$ GeV and $|\eta| < 2.2$. For Λ ’s and $\bar{\Lambda}$ ’s, the proton (pion) mass is assigned to the daughter track with larger (smaller) momentum. This assignment is nearly always correct because the decay $\Lambda \rightarrow p\pi^-$ is barely above threshold. We require that the V^0 daughter tracks not be identified as a muon. An example of an invariant mass distribution $M(\Lambda \rightarrow p\pi^-)$ is presented in Fig. 1. The D0 detector $|y|$ acceptance is narrower than the lambda production rapidity plateau as shown in Fig. 2.

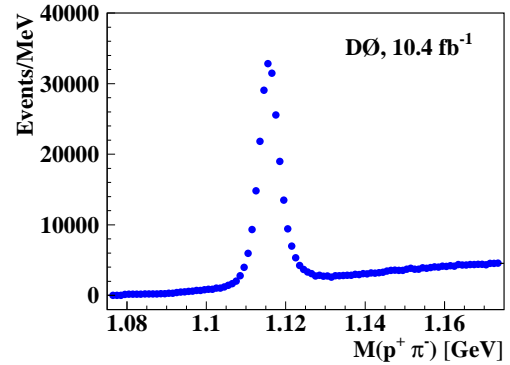


FIG. 1: Invariant mass distribution of $\Lambda \rightarrow p\pi^-$ candidates for $0.0 < y < 1.0$, muon charge $q = +1$, solenoid magnet polarity -1 , and toroid magnet polarity -1 , for the $p\bar{p} \rightarrow \mu^\pm\Lambda(\bar{\Lambda})X$ data. Other selection requirements are given in the text.

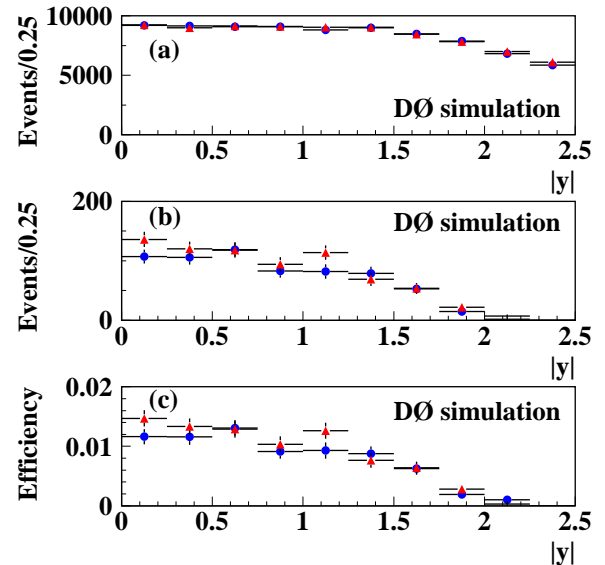


FIG. 2: (color online) Distributions of (a) generated and (b) reconstructed Λ ’s (blue circles) and $\bar{\Lambda}$ ’s (red triangles), and (c) the corresponding efficiencies, for $p_T > 2.0$ GeV, from QCD simulations of inclusive $p\bar{p}$ collisions containing a minimum parton transverse energy $E_T^{\min} > 20$ GeV. For details of the simulation see Ref. [12].

Control samples with K_S are analyzed in the same manner as the corresponding sets with Λ or $\bar{\Lambda}$, except that the track with larger momentum is assigned the pion mass instead of the proton mass. Note that we count the decays $K_S \rightarrow \pi^+\pi^-$ and $K_S \rightarrow \pi^-\pi^+$ separately, where the first pion has the larger total momentum. This way the former decay has kinematics similar to Λ decays, while the latter is similar to $\bar{\Lambda}$ decays. The $p\bar{p}$

collisions produce K^0 's and \bar{K}^0 's that we observe as resonances in invariant mass distributions of $K_S \rightarrow \pi^+\pi^-$ decays. Since this final state does not distinguish the parent K^0 from \bar{K}^0 (neglecting CP violation), K_S decays do not distinguish the p and \bar{p} directions, have no physics asymmetries, and so constitute a control sample to study detector effects.

III. RAW ASYMMETRIES AND DETECTOR EFFECTS

We observe Λ 's and $\bar{\Lambda}$'s through their decays $\Lambda \rightarrow p\pi^-$ and $\bar{\Lambda} \rightarrow \bar{p}\pi^+$. We obtain the numbers $N_F(\Lambda)$ and $N_B(\Lambda)$ [$N_F(\bar{\Lambda})$ and $N_B(\bar{\Lambda})$] of reconstructed Λ 's [$\bar{\Lambda}$'s] in the “forward” and “backward” categories, respectively, in each bin of $|y|$, by counting Λ [$\bar{\Lambda}$] candidates in the signal region (with invariant mass in the range 1.1067 to 1.1247 GeV) and subtracting the corresponding counts in two side band regions (1.0927 to 1.1017 GeV, and 1.1297 to 1.1387 GeV). These four numbers define the normalization N and three raw asymmetries A'_{FB} , A'_{NS} , and $A'_{\Lambda\bar{\Lambda}}$:

$$\begin{aligned} N_F(\Lambda) &\equiv N(1 + A'_{FB})(1 - A'_{NS})(1 + A'_{\Lambda\bar{\Lambda}}), \\ N_B(\Lambda) &\equiv N(1 - A'_{FB})(1 + A'_{NS})(1 + A'_{\Lambda\bar{\Lambda}}), \\ N_F(\bar{\Lambda}) &\equiv N(1 + A'_{FB})(1 + A'_{NS})(1 - A'_{\Lambda\bar{\Lambda}}), \\ N_B(\bar{\Lambda}) &\equiv N(1 - A'_{FB})(1 - A'_{NS})(1 - A'_{\Lambda\bar{\Lambda}}). \end{aligned} \quad (2)$$

The asymmetry A'_{NS} measures the relative excess of reconstructed Λ 's plus $\bar{\Lambda}$'s with longitudinal momentum in the \bar{p} direction (north) with respect to the p direction (south). The asymmetry $A'_{\Lambda\bar{\Lambda}}$ measures the relative excess of reconstructed Λ 's with respect to $\bar{\Lambda}$'s. The raw asymmetries A'_{FB} , A'_{NS} , and $A'_{\Lambda\bar{\Lambda}}$ defined in Eq. (2) have contributions from the physical processes of the $p\bar{p}$ collisions (A_{FB} , A_{NS} , and $A_{\Lambda\bar{\Lambda}}$, respectively), and from detector effects. As we discuss below, the raw asymmetries A'_{NS} and $A'_{\Lambda\bar{\Lambda}}$ are dominated by detector effects, while A'_{FB} is due to the physics of the $p\bar{p}$ collisions with negligible contributions from detector effects. Up to second order terms in the asymmetries, we have,

$$\begin{aligned} A'_{FB} &= \frac{N_F(\Lambda) - N_B(\Lambda) + N_F(\bar{\Lambda}) - N_B(\bar{\Lambda})}{N_F(\Lambda) + N_B(\Lambda) + N_F(\bar{\Lambda}) + N_B(\bar{\Lambda})} \\ &\quad + A'_{NS}A'_{\Lambda\bar{\Lambda}}, \\ A'_{NS} &= \frac{-N_F(\Lambda) + N_B(\Lambda) + N_F(\bar{\Lambda}) - N_B(\bar{\Lambda})}{N_F(\Lambda) + N_B(\Lambda) + N_F(\bar{\Lambda}) + N_B(\bar{\Lambda})} \\ &\quad + A'_{FB}A'_{\Lambda\bar{\Lambda}}, \\ A'_{\Lambda\bar{\Lambda}} &= \frac{N_F(\Lambda) + N_B(\Lambda) - N_F(\bar{\Lambda}) - N_B(\bar{\Lambda})}{N_F(\Lambda) + N_B(\Lambda) + N_F(\bar{\Lambda}) + N_B(\bar{\Lambda})} \\ &\quad + A'_{FB}A'_{NS}. \end{aligned} \quad (3)$$

The initial $p\bar{p}$ state is invariant with respect to CP-conjugation. Note that CP-conjugation changes the signs of A_{NS} and $A_{\Lambda\bar{\Lambda}}$, while A_{FB} is left unchanged. A non-zero A_{NS} or $A_{\Lambda\bar{\Lambda}}$ would indicate CP-violation.

The raw asymmetry A'_{NS} is different from zero if the north half of the D0 detector has a different acceptance times efficiency than the south half of the detector. This detector asymmetry does not modify A'_{FB} or $A'_{\Lambda\bar{\Lambda}}$ as defined in Eq. (2).

Antiprotons have a larger inelastic cross section with the detector material than protons. This difference results in a higher detection efficiency for Λ 's than $\bar{\Lambda}$'s. This difference in efficiencies modifies $A'_{\Lambda\bar{\Lambda}}$ but does not modify A'_{FB} or A'_{NS} as defined in Eq. (2).

The solenoid and toroid magnet polarities are reversed approximately every two weeks during data taking so that at each of the four solenoid-toroid polarity combinations approximately the same number of events are collected. The raw asymmetries obtained with each magnet polarity show variations of up to ± 0.004 for A'_{FB} , ± 0.008 for A'_{NS} , and ± 0.003 for $A'_{\Lambda\bar{\Lambda}}$. Consider an event with $\Lambda \rightarrow p\pi^-$, and the charge-conjugate (C) event with $\bar{\Lambda} \rightarrow \bar{p}\pi^+$, with the same momenta for all corresponding tracks. Assume that, due to some detector geometric effect, the former event has a larger acceptance times efficiency than the latter event for a given solenoid and toroid polarity. Now reverse these polarities. The tracks of the event $\Lambda \rightarrow p\pi^-$ with one solenoid and toroid polarity coincide with the tracks of the event $\bar{\Lambda} \rightarrow \bar{p}\pi^+$ with the opposite polarities. So with reversed polarities it is now the event with $\bar{\Lambda} \rightarrow \bar{p}\pi^+$ that has the larger acceptance times efficiency. The conjugation $\Lambda \leftrightarrow \bar{\Lambda}$ reverses the signs of A'_{FB} and $A'_{\Lambda\bar{\Lambda}}$, and leaves A'_{NS} unchanged. We conclude that by collecting equal numbers of Λ plus $\bar{\Lambda}$ for each solenoid and toroid magnet polarity combination, geometrical detector effects are canceled for A'_{FB} and $A'_{\Lambda\bar{\Lambda}}$, but not for A'_{NS} (if C symmetry holds). We weight events for each polarity combination to achieve these cancellations.

We correct A'_{NS} using the measurements with K_S by setting $A_{NS} = A'_{NS} - A'_{NS}(K_S)$. None of the detector effects discussed above affects A'_{FB} as defined in Eq. (2), so we set $A'_{FB} = A_{FB}$ (as a cross-check we verify this equality with K_S , i.e. $A'_{FB}(K_S) = 0$ within statistical uncertainties). We do not measure $A_{\Lambda\bar{\Lambda}}$ as we are not able to separate the effect due to different reconstruction efficiencies from the raw asymmetry $A'_{\Lambda\bar{\Lambda}}$.

IV. RESULTS FOR MINIMUM BIAS EVENTS

We now consider minimum bias events $p\bar{p} \rightarrow \Lambda(\bar{\Lambda})X$ and the control sample $p\bar{p} \rightarrow K_S X$. Distributions of p_T , p_z , and y of reconstructed Λ 's and $\bar{\Lambda}$'s are shown in Fig. 3. The raw asymmetries of Λ , $\bar{\Lambda}$ and K_S for $p_T > 2.0$ GeV are presented in Fig. 4. We expect the asymmetries $A'_{FB}(K_S)$ and $A'_{\Lambda\bar{\Lambda}}(K_S)$ to be zero, while $A'_{NS}(K_S)$ is not necessarily zero. These expectations are satisfied within the statistical uncertainties. From Fig. 4 (c) we obtain $A'_{\Lambda\bar{\Lambda}} \approx 0.022$. This asymmetry is different from zero as expected from the different inelastic cross-sections of p and \bar{p} , and of Λ and $\bar{\Lambda}$, with the detector

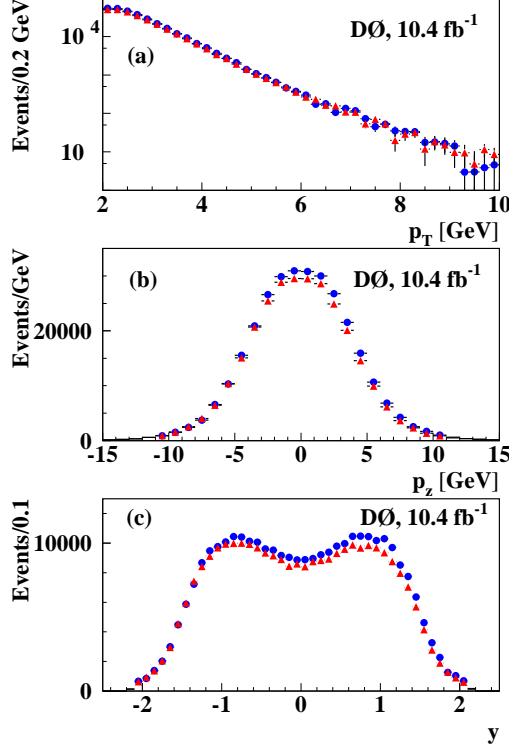


FIG. 3: (color online) Distributions of (a) p_T , (b) p_z , and (c) y of reconstructed Λ 's (blue circles) and $\bar{\Lambda}$'s (red triangles) with $p_T > 2.0$ GeV, for the minimum bias data sample $p\bar{p} \rightarrow \Lambda(\bar{\Lambda})X$.

material. The asymmetries in Fig. 4 were obtained from Eqs. (3) but neglecting the quadratic terms. Therefore the forward-backward asymmetries shown in Fig. 4 need corrections $A'_{NS}A'_{\Lambda\bar{\Lambda}}$ due to detector effects. These corrections, obtained bin-by-bin from Fig. 4 (b) and (c), are measured to be consistent with zero within their statistical uncertainties. As they are small, they are not applied as corrections, but are treated as systematic uncertainties. They vary from ± 0.0001 for the first bin of $|y|$ to ± 0.0004 for the $1.5 < |y| < 1.75$ bin. The results for A_{FB} are presented in Fig. 4 and Table II. The corrected asymmetry $A_{NS} = A'_{NS} - A'_{NS}(K_S)$ is consistent with zero within the statistical uncertainties, so we observe no significant CP violation in A_{NS} , as shown in Fig. 5.

In Figs. 6 and 7, the asymmetry A_{FB} shown in Fig. 4 is compared with other experiments that study collisions $pZ \rightarrow \Lambda(\bar{\Lambda})X$ for several targets $Z = p, \bar{p}, \text{Be and Pb}$. For the D0 minimum bias data in Figs. 6 and 7, we plot $[\sigma_B(\Lambda) + \sigma_B(\bar{\Lambda})]/[\sigma_F(\Lambda) + \sigma_F(\bar{\Lambda})] = (1 - A_{FB})/(1 + A_{FB})$. We should note that the point $y = 0$ in the center of mass for $p\bar{p}$ collisions has a $\bar{\Lambda}/\Lambda$ production ratio equal to 1 if CP is conserved, which is not necessarily the case for pp collisions, so this D0 point at large rapidity loss should be excluded from the comparison with pp data. From Figs. 6 and 7 we conclude that the $\bar{\Lambda}/\Lambda$ production ratio is

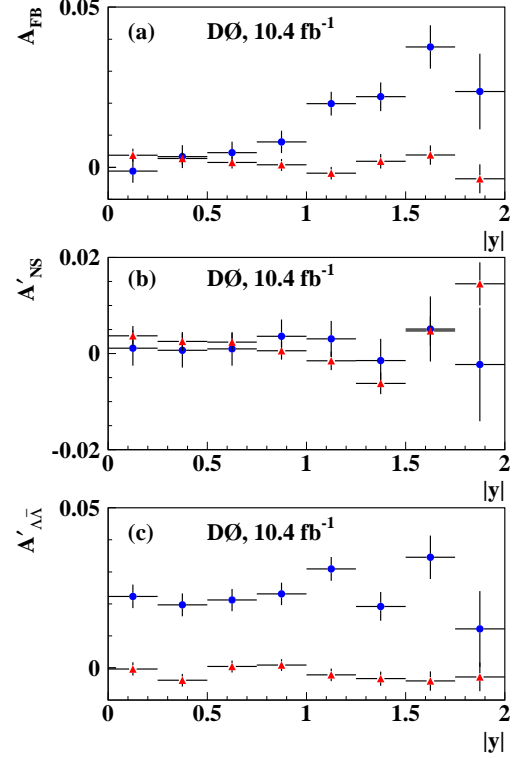


FIG. 4: (color online) Asymmetries (a) $A_{FB} = A'_{FB}$, (b) A'_{NS} , and (c) $A'_{\Lambda\bar{\Lambda}}$ of reconstructed Λ and $\bar{\Lambda}$ (blue circles) and K_S (red triangles) with $p_T > 2.0$ GeV, as functions of $|y|$, for the minimum bias data samples $p\bar{p} \rightarrow \Lambda(\bar{\Lambda})X$ or $p\bar{p} \rightarrow K_S X$ respectively. Uncertainties are statistical.

approximately a universal function of the “rapidity loss” $\Delta y \equiv y_p - y$, independent of \sqrt{s} or target Z . Here y_p is the rapidity of the proton beam, and y is the rapidity of the Λ or $\bar{\Lambda}$.

V. RESULTS FOR EVENTS WITH A J/ψ OR A MUON

The results of the measurements with the data set $p\bar{p} \rightarrow J/\psi \Lambda(\bar{\Lambda})X$ are presented in Fig. 8 and Table II. We note that A_{NS} is consistent with zero, whereas A_{FB} is significantly nonzero at large $|y|$.

We now consider the large data sample $p\bar{p} \rightarrow \mu^\pm \Lambda(\bar{\Lambda})X$. Rapidity distributions for reconstructed Λ 's and $\bar{\Lambda}$'s are presented in Fig. 9. After accounting for the different efficiencies to detect Λ and $\bar{\Lambda}$, we find that there are more events $\Lambda\mu^+$ and $\bar{\Lambda}\mu^-$, than events $\Lambda\mu^-$ and $\bar{\Lambda}\mu^+$. Examples of decays with a $\Lambda\mu^+$ correlation are: $\Lambda_c^+ \rightarrow \Lambda\mu^+\nu_\mu$ and $p\bar{p} \rightarrow \Lambda K^+ X$ followed by $K^+ \rightarrow \mu^+\nu_\mu$ (note that the Λ and K^+ share an $s\bar{s}$ pair). The reverse $\Lambda\mu^-$ correlation occurs for $\Lambda_b \rightarrow \mu^-\Lambda_c^+\bar{\nu}_\mu X$ with $\Lambda_c^+ \rightarrow \Lambda X$. Measurements of $A_{FB}(|y|)$ for events with μ^+ or μ^- are found to be consistent within statistical

TABLE II: Forward-backward asymmetry A_{FB} of Λ and $\bar{\Lambda}$ with $p_T > 2.0$ GeV in minimum bias events $p\bar{p} \rightarrow \Lambda(\bar{\Lambda})X$, events $p\bar{p} \rightarrow J/\psi\Lambda(\bar{\Lambda})X$, and events $p\bar{p} \rightarrow \mu^\pm\Lambda(\bar{\Lambda})X$. The first uncertainty is statistical, the second is systematic.

$ y $	$A_{FB} \times 100$ (min. bias)	$A_{FB} \times 100$ (with J/ψ)	$A_{FB} \times 100$ (with μ)
0.00 to 0.25	$-0.12 \pm 0.37 \pm 0.01$	$-0.21 \pm 0.58 \pm 0.01$	$0.16 \pm 0.09 \pm 0.02$
0.25 to 0.50	$0.33 \pm 0.36 \pm 0.01$	$0.10 \pm 0.57 \pm 0.02$	$0.24 \pm 0.09 \pm 0.02$
0.50 to 0.75	$0.45 \pm 0.35 \pm 0.01$	$0.69 \pm 0.56 \pm 0.02$	$0.67 \pm 0.08 \pm 0.02$
0.75 to 1.00	$0.79 \pm 0.35 \pm 0.02$	$0.55 \pm 0.56 \pm 0.02$	$0.85 \pm 0.08 \pm 0.02$
1.00 to 1.25	$1.99 \pm 0.37 \pm 0.02$	$0.69 \pm 0.59 \pm 0.03$	$1.57 \pm 0.09 \pm 0.02$
1.25 to 1.50	$2.20 \pm 0.45 \pm 0.02$	$1.72 \pm 0.72 \pm 0.03$	$1.98 \pm 0.10 \pm 0.04$
1.50 to 1.75	$3.75 \pm 0.68 \pm 0.03$	$3.24 \pm 1.12 \pm 0.06$	$2.53 \pm 0.16 \pm 0.06$
1.75 to 2.00	$2.37 \pm 1.18 \pm 0.04$	$2.64 \pm 2.06 \pm 0.06$	$3.11 \pm 0.30 \pm 0.06$

TABLE III: Forward-backward asymmetry A_{FB} of Λ and $\bar{\Lambda}$ in bins of p_T in events $p\bar{p} \rightarrow \mu^\pm\Lambda(\bar{\Lambda})X$. The first uncertainty is statistical, the second is systematic.

$ y $	$A_{FB} \times 100$ $2 < p_T < 4$ GeV	$A_{FB} \times 100$ $4 < p_T < 6$ GeV	$A_{FB} \times 100$ $p_T > 6$ GeV
0.00 to 0.25	$0.21 \pm 0.09 \pm 0.02$	$-0.27 \pm 0.28 \pm 0.02$	$0.57 \pm 0.69 \pm 0.02$
0.25 to 0.50	$0.25 \pm 0.09 \pm 0.02$	$0.20 \pm 0.27 \pm 0.02$	$-0.47 \pm 0.63 \pm 0.02$
0.50 to 0.75	$0.70 \pm 0.08 \pm 0.02$	$0.50 \pm 0.26 \pm 0.02$	$1.11 \pm 0.58 \pm 0.02$
0.75 to 1.00	$0.82 \pm 0.08 \pm 0.02$	$1.02 \pm 0.25 \pm 0.02$	$0.57 \pm 0.54 \pm 0.02$
1.00 to 1.25	$1.60 \pm 0.10 \pm 0.02$	$1.39 \pm 0.25 \pm 0.02$	$2.38 \pm 0.52 \pm 0.02$
1.25 to 1.50	$1.94 \pm 0.11 \pm 0.04$	$2.17 \pm 0.27 \pm 0.04$	$2.43 \pm 0.57 \pm 0.04$
1.50 to 1.75	$2.61 \pm 0.17 \pm 0.06$	$2.10 \pm 0.42 \pm 0.06$	$4.77 \pm 0.85 \pm 0.06$
1.75 to 2.00	$3.05 \pm 0.32 \pm 0.06$	$3.49 \pm 0.83 \pm 0.06$	$6.32 \pm 1.69 \pm 0.06$

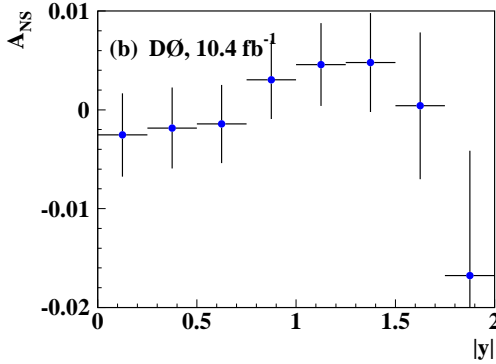


FIG. 5: Corrected asymmetry $A_{NS} = A'_{NS} - A'_{NS}(K_S)$ of Λ and $\bar{\Lambda}$ with $p_T > 2.0$ GeV, as a function of $|y|$, for the minimum bias data sample $p\bar{p} \rightarrow \Lambda(\bar{\Lambda})X$. Uncertainties are statistical.

uncertainties, so we combine events with μ^+ and μ^- and obtain the results presented in Fig. 10. We assign to A_{FB} a systematic uncertainty equal to the entire detector effect, $A'_{NS}A'_{\Lambda\bar{\Lambda}}$. Numerical results are presented in Table II. The forward-backward asymmetry A_{FB} as a function of $|y|$ for different lambda transverse momentum bins is shown in Fig. 11 and Table III. Note that A_{FB} is only weakly dependent on $p_T(\Lambda)$.

The final results of this analysis are summarized in Tables II and III, and Figs. 11 and 12.

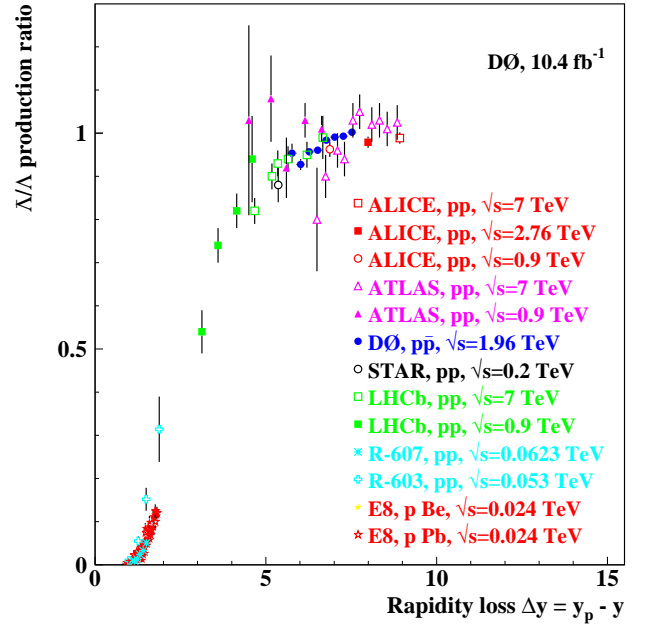


FIG. 6: $\bar{\Lambda}/\Lambda$ production ratio as a function of the rapidity loss $\Delta y \equiv y_p - y$ for several experiments that study reactions $pZ \rightarrow \Lambda(\bar{\Lambda})X$ for targets $Z = p, \bar{p}, \text{Be}$ and Pb . The experiments are ALICE [13], ATLAS [14], DØ (this analysis), STAR [15], LHCb [16], ISR R-607 [17], ISR R-603 [18], and the fixed target experiment Fermilab E8 studying $p\text{-Be}$ and $p\text{-Pb}$ collisions at a beam energy of 300 GeV [19].

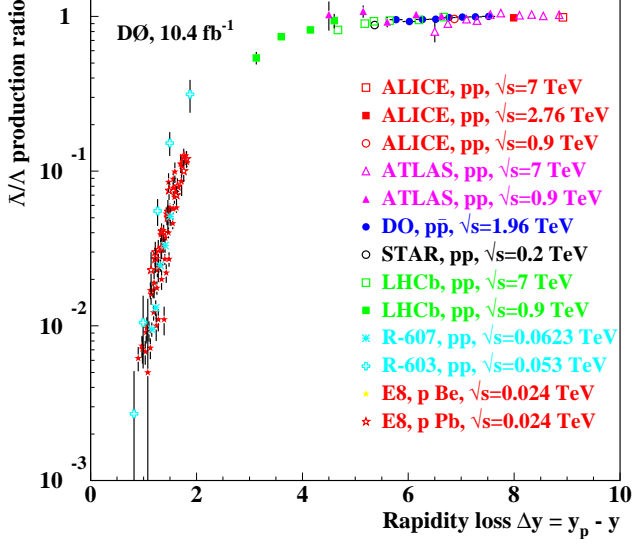


FIG. 7: Same as Fig. 6 with logarithmic scale.

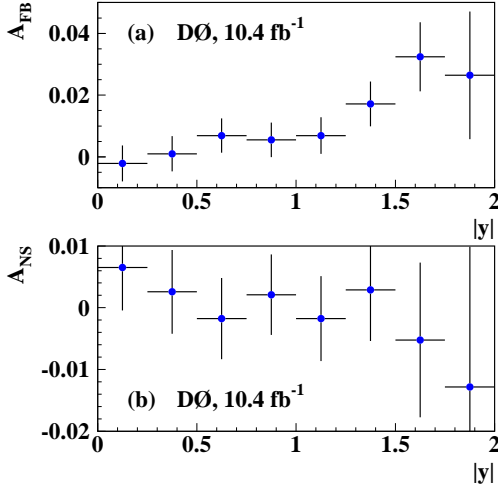


FIG. 8: Asymmetries (a) $A_{FB} = A'_{FB}$ and (b) $A_{NS} = A'_{NS} - A'_{NS}(K_S)$ of Λ and $\bar{\Lambda}$ with $p_T > 2.0$ GeV, as functions of $|y|$, for the data sample $p\bar{p} \rightarrow J/\psi\Lambda(\bar{\Lambda})X$. Uncertainties are statistical.

VI. CONCLUSIONS

We have measured the forward-backward asymmetry of Λ and $\bar{\Lambda}$ production A_{FB} as a function of rapidity $|y|$ for three data sets: $p\bar{p} \rightarrow \Lambda(\bar{\Lambda})X$, $p\bar{p} \rightarrow J/\psi\Lambda(\bar{\Lambda})X$, and $p\bar{p} \rightarrow \mu^\pm\Lambda(\bar{\Lambda})X$. The asymmetry A_{FB} is a function of $|y|$ that does not depend significantly on the data set or data composition (see Fig. 12), and is weakly dependent on p_T (see Fig. 11). The measurement of A_{FB} in $p\bar{p}$ collisions can be compared with the $\bar{\Lambda}/\Lambda$ production ratio mea-

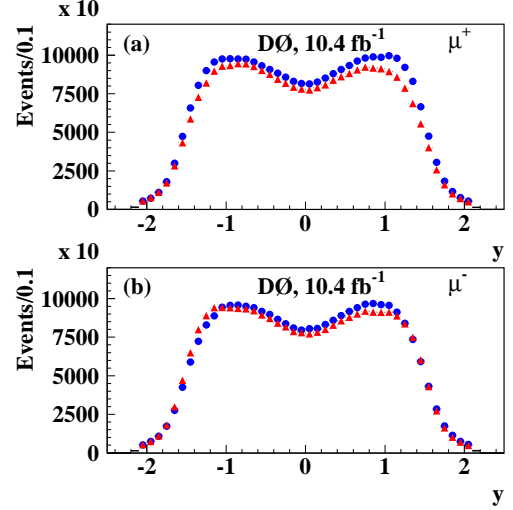


FIG. 9: (color online) Distributions of rapidity y of reconstructed Λ 's (blue circles) and $\bar{\Lambda}$'s (red triangles) for events with (a) μ^+ or (b) μ^- , for $p_T > 2.0$ GeV, for events $p\bar{p} \rightarrow \mu^\pm\Lambda(\bar{\Lambda})X$.

sured by a wide range of proton scattering experiments. This production ratio is confirmed to be approximately a universal function of the “rapidity loss” $y_p - y$, that does not depend significantly (or depends only weakly) on the total center of mass energy \sqrt{s} or target (see Figs. 6 and 7). This result supports the view that a strange quark produced directly in the hard scattering of point-like partons, or indirectly in the subsequent showering, can coalesce with a diquark remnant of the beam particle to produce a lambda with a probability that increases as the rapidity difference between the proton and lambda decreases.

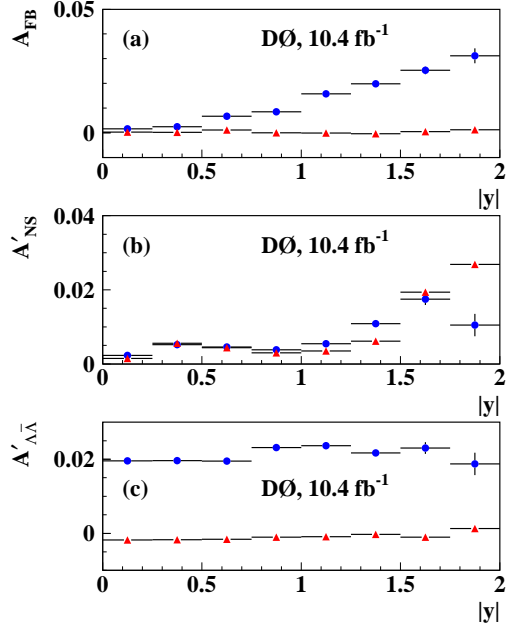


FIG. 10: (color online) Asymmetries (a) $A_{FB} = A'_{FB}$, (b) A'_{NS} , and (c) $A'_{\Lambda\bar{\Lambda}}$ of reconstructed Λ and $\bar{\Lambda}$ (blue circles) and K_S (red triangles) with $p_T > 2.0$ GeV, as functions of $|y|$, for events $p\bar{p} \rightarrow \mu^\pm \Lambda(\bar{\Lambda}) X$ or $p\bar{p} \rightarrow \mu^\pm K_S X$ respectively. Uncertainties are statistical.

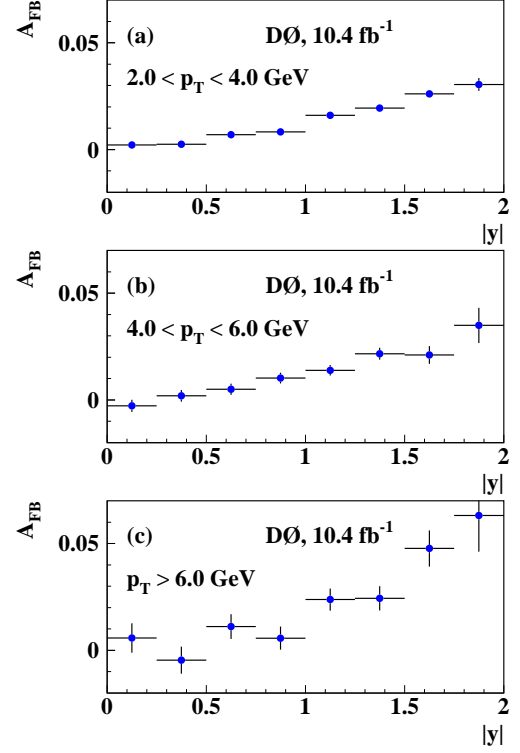


FIG. 11: Asymmetry A_{FB} as a function of $|y|$ for events $p\bar{p} \rightarrow \mu^\pm \Lambda(\bar{\Lambda}) X$ for (a) $2.0 < p_T < 4.0$ GeV, (b) $4.0 < p_T < 6.0$ GeV, and (c) $p_T > 6.0$ GeV. Uncertainties are statistical.

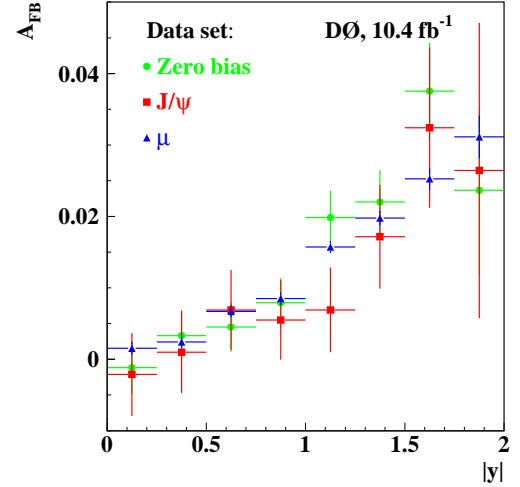


FIG. 12: (color online) Asymmetry A_{FB} as a function of $|y|$ for events $p\bar{p} \rightarrow \Lambda(\bar{\Lambda}) X$ (green circles), $p\bar{p} \rightarrow J/\psi \Lambda(\bar{\Lambda}) X$ (red squares), and $p\bar{p} \rightarrow \mu^\pm \Lambda(\bar{\Lambda}) X$ (blue triangles) for $p_T > 2.0$ GeV. Uncertainties are statistical.

Acknowledgments

We thank the staffs at Fermilab and collaborating institutions, and acknowledge support from the Department of Energy and National Science Foundation (United States of America); Alternative Energies and Atomic Energy Commission and National Center for Scientific Research/National Institute of Nuclear and Particle Physics (France); Ministry of Education and Science of the Russian Federation, National Research Center “Kurchatov Institute” of the Russian Federation, and Russian Foundation for Basic Research (Russia); National Council for the Development of Science and Technology and Carlos Chagas Filho Foundation for the Support of Research in the State of Rio de Janeiro (Brazil); Department of Atomic Energy and Department of Science and Tech-

nology (India); Administrative Department of Science, Technology and Innovation (Colombia); National Council of Science and Technology (Mexico); National Research Foundation of Korea (Korea); Foundation for Fundamental Research on Matter (The Netherlands); Science and Technology Facilities Council and The Royal Society (United Kingdom); Ministry of Education, Youth and Sports (Czech Republic); Bundesministerium für Bildung und Forschung (Federal Ministry of Education and Research) and Deutsche Forschungsgemeinschaft (German Research Foundation) (Germany); Science Foundation Ireland (Ireland); Swedish Research Council (Sweden); China Academy of Sciences and National Natural Science Foundation of China (China); and Ministry of Education and Science of Ukraine (Ukraine).

-
- [1] K. P. Das and Rudolph C. Hwa, *Quark-antiquark recombination in the fragmentation region*, Phys. Lett. B **68**, 5 (1977).
 - [2] Stanley J. Brodsky and John F. Gunion, *Hadronic fragmentation as a probe of the underlying dynamics of hadron collisions*, Phys. Rev. D **17**, 3 (1978).
 - [3] D. Cutts *et al.*, *Experimental study of low- p_t hadron fragmentation*, Phys. Rev. Lett. **43**, 5 (1979).
 - [4] Rudolph C. Hwa and R. G. Roberts, *Pion structure function from low- p_t hadron production*, Z. Physik C, **1**, 81-86 (1979) and references therein.
 - [5] V.M. Abazov *et al.* (D0 Collaboration), *The upgraded D0 detector*, Nucl. Instrum. Methods in Phys. Res. A **565**, 463 (2006).
 - [6] V.M. Abazov *et al.*, *The muon system of the Run II D0 detector*, Nucl. Instrum. Methods in Phys. Res. A **552**, 372 (2005).
 - [7] S.N. Ahmed *et al.*, (D0 Collaboration), *The D0 Silicon Microstrip Tracker*, Nucl. Instrum. Methods Phys. Res. A **634**, 8 (2011).
 - [8] R. Angstadt *et al.*, (D0 Collaboration), *The layer 0 inner silicon detector of the D0 experiment*, Nucl. Instrum. Methods Phys. Res. A **622**, 298 (2010).
 - [9] V.M. Abazov *et al.* (D0 Collaboration), *Muon reconstruction and identification with the Run II D0 detector*, Nucl. Instrum. Methods in Phys. Res. Sect. A **737**, 281 (2014).
 - [10] V. M. Abazov *et al.* (D0 Collaboration), *Study of CP-violating charge asymmetries of single muons and like-sign dimuons in $p\bar{p}$ collisions*, Phys. Rev. D **89** 012002 (2014).
 - [11] V. M. Abazov *et al.* (D0 Collaboration), *Measurement of the anomalous like-sign dimuon charge asymmetry with 9 fb^{-1} of $p\bar{p}$ collisions*, Phys. Rev. D **84**, 052007 (2011).
 - [12] V. M. Abazov *et al.* (D0 Collaboration), *Evidence for an anomalous like-sign dimuon charge asymmetry*, Phys. Rev. D **82**, 032001 (2010).
 - [13] E. Abbas *et al.* (ALICE Collaboration), *Mid-rapidity anti-baryon to baryon ratios in pp collisions at $\sqrt{s} = 0.9, 2.76$, and 7 TeV measured by ALICE*, Eur. Phys. J. C **73**, 2496 (2013).
 - [14] G. Aad *et al.* (ATLAS Collaboration), *K_S^0 and Λ production in pp interactions at $\sqrt{s} = 0.9$ and 7 TeV measured with the ATLAS detector at the LHC*, Phys. Rev. D **85** (2012) 012001.
 - [15] B.I. Abelev *et al.* (STAR Collaboration), *Strange particle production in p + p collisions at $\sqrt{s} = 200$ GeV*, Phys. Rev. C **75**, 064901 (2007).
 - [16] R. Aaij *et al.* (LHCb Collaboration), *Measurement of V^0 production ratios in pp collisions at $\sqrt{s} = 0.9$ and 7 TeV*, J. High Energy Phys. **1108** (2011) 034.
 - [17] G.J. Bobbink *et al.* (R-607 Collaboration), *The production of high-momentum particles and resonances in pp collisions at the CERN intersecting storage rings*, Nucl. Phys. B **217** (1983) 11.
 - [18] S. Erhan *et al.* (R-603 Collaboration), *Hyperon production in pp interactions at $\sqrt{s} = 53$ and 62 GeV*, Phys. Lett. B **85** (1979) 447.
 - [19] P. Skubic *et al.* (E8 Collaboration), *Neutral-strange-particle production by 300-GeV protons*, Phys. Rev. D **18**, 3115 (1978).